

# Magnetic properties of $\text{EuTiO}_3$ , $\text{Eu}_2\text{TiO}_4$ , and $\text{Eu}_3\text{Ti}_2\text{O}_7$ <sup>†</sup>

Chia-Ling Chien\* and S. DeBenedetti

Department of Physics, Carnegie-Mellon University, Pittsburgh, Pennsylvania 15213

F. De S. Barros

Instituto de Fisica, Universidade Federal do Rio de Janeiro, Rio de Janeiro, GB, Brazil

(Received 8 April 1974)

We have investigated the magnetic properties of  $\text{EuTiO}_3$  ( $T_N = 5.3 \pm 0.2$  K),  $\text{Eu}_2\text{TiO}_4$  ( $T_C = 7.8 \pm 0.2$  K), and  $\text{Eu}_3\text{Ti}_2\text{O}_7$  ( $T_C = 8 \pm 0.3$  K) with the technique of  $^{151}\text{Eu}$  Mössbauer spectroscopy. The magnetic exchange constants of these substances were obtained from the spectra using molecular-field theory and were interpreted in terms of  $5d$  admixtures to the  $4f$  wave functions of the  $\text{Eu}^{2+}$  ion. In  $\text{Eu}_3\text{Ti}_2\text{O}_7$ , we have found two magnetic inequivalent sites, with different temperature dependence of the sublattice magnetization. The quadrupole moment ratio of the 21.6-keV state to the ground state of  $^{151}\text{Eu}$  was measured to be  $1.34 \pm 0.03$  using  $\text{Eu}_2\text{TiO}_4$ , which has an axially symmetric electric field gradient ( $\eta = 0$ ) at the Eu sites. A calculation of the splitting of the admixed  $5d$  electronic levels and of the electric field gradient at the nucleus was performed by summing the lattice contributions with the method of chargeless cluster. The results provided an interpretation of the magnetic properties and of the nuclear quadrupole interaction in the substances studied.

## I. INTRODUCTION

The magnetic properties of  $\text{Eu}^{2+}$  compounds have been the subject of many investigations ever since  $\text{EuO}$  was found to be ferromagnetic below 70 K.<sup>1</sup>

The first known ternary compound of  $\text{Eu}^{2+}$  belonging to the Eu-Ti-O system was  $\text{EuTiO}_3$ ,<sup>2</sup> and a number of other compounds of this type were identified in 1969 by McCarthy *et al.*,<sup>3</sup> while studying the phase relations of the Eu-Ti-O system.

In the present paper we discuss the magnetic properties of  $\text{EuTiO}_3$ ,  $\text{Eu}_2\text{TiO}_4$ , and  $\text{Eu}_3\text{Ti}_2\text{O}_7$ . We shall also report some studies on a solid solution  $\text{EuTiO}_x$  ( $2.5 \leq x \leq 3$ ).

These substances were investigated with the technique of Mössbauer spectroscopy, using the 21.6-keV  $\gamma$  rays of  $^{151}\text{Eu}$ . Since spin relaxation times are short in concentrated samples, we assumed that the hyperfine fields  $H_{\text{hf}}$ , obtained from the spectra, had the same temperature dependence as the sublattice magnetization; and, since the Mössbauer effect is a microscopic probe, we were then able to follow the sublattice magnetizations of several inequivalent sites. From the temperature dependence of the sublattice magnetizations, we could derive the value of the corresponding magnetic exchange constants.

We have also determined the quadrupole moment ratio  $R = Q_1(21.6 \text{ keV})/Q_0$  of the  $^{151}\text{Eu}$  nucleus using samples of  $\text{Eu}_2\text{TiO}_4$ , which have a convenient transition temperature and an axially symmetrical electric field gradient (EFG) tensor.

## II. CRYSTAL STRUCTURE AND MAGNETIC INTERACTIONS

$\text{EuTiO}_3$  crystallizes with a cubic perovskite structure with a lattice parameter of 3.90 Å

(Fig. 1).<sup>2,3</sup> The magnetic  $\text{Eu}^{2+}$  site is cubic.

X-ray studies<sup>3</sup> have shown that the oxygen-deficient solid solutions  $\text{EuTiO}_x$  ( $2.5 \leq x \leq 3$ ) have the same cell parameter (3.9 Å) for the entire range of  $x$  and have given no evidence of distortion from cubic symmetry.

The crystal structure of  $\text{Eu}_2\text{TiO}_4$  is of  $\text{K}_2\text{NiF}_4$  type with space group  $D_{4h}^{17}$  ( $I4/mmm$ ) (Fig. 1). The tetragonal unit cell with cell parameters<sup>3</sup>  $a = 3.883$  Å and  $c = 12.523$  Å contains two formula units. An important feature of the  $\text{Eu}^{2+}$  point symmetry is the presence of a fourfold rotation axis ( $c$  axis).

$\text{Eu}_3\text{Ti}_2\text{O}_7$  with space group  $D_{4h}^1 = I4/mmm$ , cell parameters<sup>3</sup>  $a = 3.90$  Å and  $c = 20.28$  Å, can be visualized as composed of alternate layers of  $\text{EuTiO}_3$  and  $\text{Eu}_2\text{TiO}_4$  (Fig. 1). There are two non-equivalent  $\text{Eu}^{2+}$  sites with the same local environment as in  $\text{Eu}_2\text{TiO}_4$  and  $\text{EuTiO}_3$  ( $\text{Eu}_2\text{TiO}_4$  site and  $\text{EuTiO}_3$  site). The  $\text{Eu}_2\text{TiO}_4$  sites are twice as many as the  $\text{EuTiO}_3$  sites.

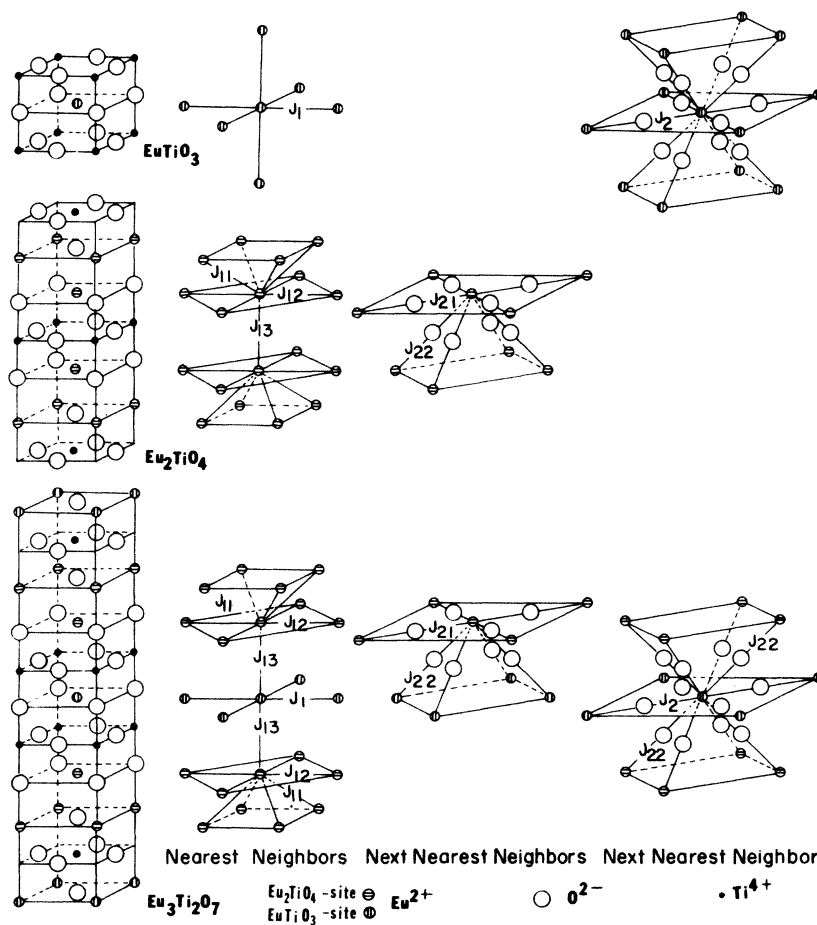
In the analysis of the magnetic properties of  $\text{EuTiO}_3$ ,  $\text{Eu}_2\text{TiO}_4$ , and  $\text{Eu}_3\text{Ti}_2\text{O}_7$ , only nearest neighbor (nn) and next nearest neighbor (nnn) were considered, within the framework of the molecular-field theory.

The nn's are at a distance of about 3.9 Å and the nnn's are at a distance of about 5.5 Å in all these compounds. The magnetic interaction is direct for nn, and indirect, via superexchange through the  $\text{O}^{2-}$  ions for nnn, as shown in Fig. 1 and Table I. In  $\text{Eu}_2\text{TiO}_4$  and  $\text{Eu}_3\text{Ti}_2\text{O}_7$ , there are more than one type of nn and nnn exchange interactions; therefore double-indexed  $J$ 's are used.

The  $\text{Eu}^{2+}$  free ion with a  $4f^7$  electronic configuration is in a spherically symmetric  $^8S_{7/2}$  state.

TABLE I. Exchange interactions of  $\text{EuTiO}_3$ ,  $\text{Eu}_2\text{TiO}_4$ , and  $\text{Eu}_3\text{Ti}_2\text{O}_7$ .

Material	Exchange nn	nnn	No.	$\text{Eu}^{2+}\text{-Eu}^{2+}$ distance (Å)	Direction <sup>a</sup>	Connecting 5d orbitals
$\text{EuTiO}_3$	$J_1$	...	6	3.90	$\langle 100 \rangle$	$ 3z^2 - r^2\rangle,  x^2 - y^2\rangle$
	...	$J_2$	12	5.51	$\langle 110 \rangle$	$ xy\rangle,  yz\rangle,  zx\rangle$
$\text{Eu}_2\text{TiO}_4$	$J_{11}$	...	4	3.75	$\sim \langle 11\sqrt{2} \rangle$	$( xy\rangle +  yz\rangle)$
	$J_{12}$	...	4	3.88	$\langle 100 \rangle$	$ x^2 - y^2\rangle$
	$J_{13}$	...	1	3.81	$\langle 001 \rangle$	$ 3z^2 - r^2\rangle$
	...	$J_{21}$	4	5.49	$\langle 110 \rangle$	$ xy\rangle$
	...	$J_{22}$	4	5.44	$\sim \langle 101 \rangle$	$ xz\rangle,  yz\rangle$
EuTiO <sub>3</sub> site of Eu <sub>3</sub> Ti <sub>2</sub> O <sub>7</sub>	$J_1$	...	4	3.90	$\langle 100 \rangle$	$ x^2 - y^2\rangle$
	$J_{13}$	...	2	3.81	$\langle 001 \rangle$	$ 3z^2 - r^2\rangle$
Eu <sub>3</sub> Ti <sub>2</sub> O <sub>7</sub>	...	$J_2$	4	5.51	$\langle 110 \rangle$	$ xy\rangle$
	...	$J_{22}$	8	5.45	$\sim \langle 101 \rangle$	$ xz\rangle,  yz\rangle$
Eu <sub>2</sub> TiO <sub>4</sub> site of Eu <sub>3</sub> Ti <sub>2</sub> O <sub>7</sub>	$J_{11}$	...	4	3.74	$\sim \langle 11\sqrt{2} \rangle$	$( xy\rangle +  yz\rangle)$
	$J_{12}$	...	4	3.88	$\langle 100 \rangle$	$ x^2 - y^2\rangle$
	$J_{13}$	...	1	3.81	$\langle 001 \rangle$	$ 3z^2 - r^2\rangle$
Eu <sub>3</sub> Ti <sub>2</sub> O <sub>7</sub>	...	$J_{21}$	4	5.5	$\langle 110 \rangle$	$ xy\rangle$
	...	$J_{22}$	4	5.45	$\sim \langle 101 \rangle$	$ xz\rangle,  yz\rangle$

<sup>a</sup>Expressed in terms of direction cosines.FIG. 1. Crystal structures (1st column), nearest-neighbor interactions (2nd column), and next-nearest-neighbor interactions (3rd and 4th columns) of  $\text{EuTiO}_3$ ,  $\text{Eu}_2\text{TiO}_4$  and  $\text{Eu}_3\text{Ti}_2\text{O}_7$ .  $\text{EuTiO}_3$ -site and  $\text{Eu}_2\text{TiO}_4$ -site are denoted differently.

In a solid, the highly localized  $4f$  wave functions have little overlap with the neighboring  $\text{Eu}^{2+}$  ions;  $4f$  exchange, which favors antiferromagnetism, is then expected to contribute only very weakly to magnetic ordering.<sup>4</sup> In order to explain the finding of many ferromagnetic materials with high  $T_C$ ,<sup>5</sup> we must consider the effect of small admixtures of  $5d$  wave functions to the  $4f$  state. Such admixtures were previously introduced<sup>5,6</sup> for the interpretation of optical properties.<sup>4,7</sup>

According to this view, the dominant interaction for direct exchange has the form<sup>4</sup>

$$J_1 \sim J^{\text{intra}} b^2 / U^2, \quad (1)$$

where  $J^{\text{intra}}$  is the intra-atomic exchange parameter between the  $4f$  and  $5d$  wave functions of  $\text{Eu}^{2+}$ , roughly unchanged for different compounds,<sup>8</sup>  $b$  is the transfer integral which depends upon the distance of separation, and  $U$  is the excitation energy from the  $4f$  level to those  $5d$  sublevels which have orbitals pointing toward the nn  $\text{Eu}^{2+}$  ions.

Since for all the substances in which we are interested the separation distance is approximately the same, we will neglect the variation of  $b$ . Furthermore, since the  $5d$ - $4f$  energy difference averaged over the  $5d$  sublevels can be assumed to be the same for different compounds ( $U_0 \approx 3.5$  eV),<sup>6</sup> we can write

$$U_i = U_0 + \Delta_i, \quad (2)$$

where  $\Delta_i$  ( $i=1-5$ ) depends upon the splitting of the  $5d$  levels (Fig. 2); with the understanding that only those sublevels  $i$  with lobes in the direction of the nn  $\text{Eu}^{2+}$  are of interest for the exchange interaction.

For example, for cubic point symmetry at the  $\text{Eu}^{2+}$  site,  $i$  assumes two values:  $i = t_{2g}$  (triplet  $|xy\rangle$ ,  $|yz\rangle$ ) and  $i = e_g$  (doublet  $|x^2 - y^2\rangle$ ,  $|3z^2 - r^2\rangle$ ). The  $t_{2g}$  states, which have lobes in the  $\langle 110 \rangle$  crystal direction, are of interest for the exchange interaction when the  $\text{Eu}^{2+}$  form a face-centered cubic lattice; and the  $e_g$  states, which have lobes in the  $\langle 100 \rangle$  direction, are of interest when the  $\text{Eu}^{2+}$  form a simple cubic lattice.

Let us now define the cubic crystal-field splitting  $10Dq$  to have the sign

$$10Dq = E_{t_{2g}} - E_{e_g}. \quad (3)$$

Then, for face-centered-cubic lattices, such as  $\text{EuO}$  and  $\text{EuS}$ , for which the  $t_{2g}$  lobes point towards the nn  $\text{Eu}^{2+}$ , we can write

$$U = U_0 + \frac{2}{5} (10Dq), \quad (4)$$

and for simple cubic lattices, such as  $\text{EuTiO}_3$  and  $\text{EuLiH}_3$ , for which the lobes pointing to the nn  $\text{Eu}^{2+}$  are  $e_g$ , we have

$$U = U_0 - \frac{3}{5} (10Dq). \quad (5)$$

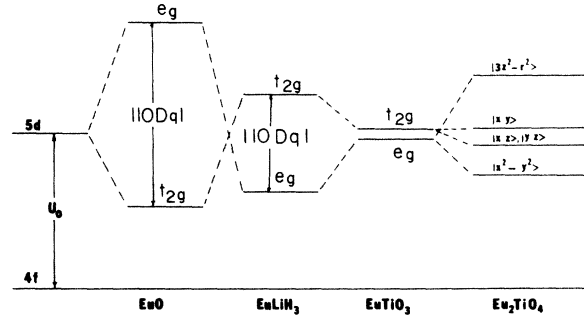


FIG. 2. Schematic  $5d$  crystal-field splitting of  $\text{EuO}$ ,  $\text{EuLiH}_3$ ,  $\text{EuTiO}_3$ , and  $\text{Eu}_2\text{TiO}_4$ .

The case of tetragonal symmetry, with only two of the five  $5d$  levels degenerate ( $|xz\rangle$  and  $|yz\rangle$ ), will be discussed in connection with  $\text{Eu}_2\text{TiO}_4$  and  $\text{Eu}_3\text{Ti}_2\text{O}_7$ .

The indirect superexchange between nnn  $\text{Eu}^{2+}$  ions, which also involves  $5d$  admixture, is much more complicated than the direct exchange mentioned above. However, since the superexchange in  $\text{Eu}^{2+}$  compounds is usually not of large magnitude,<sup>5,7</sup> we shall assume that it is the same in  $\text{Eu}_2\text{TiO}_4$ ,  $\text{Eu}_3\text{Ti}_2\text{O}_7$  as in  $\text{EuTiO}_3$ .

### III. EXPERIMENTAL

In the Mössbauer apparatus, the  $^{151}\text{Sm}_2\text{O}_3$  source emitting the 21.6-keV  $\gamma$  rays was maintained at room temperature. The source velocity was calibrated by the six-line spectrum of  $\alpha\text{-Fe}_2\text{O}_3$  using a  $^{57}\text{Co}$  source attached to the opposite end of the drive rod.

The powder samples of  $\text{EuTiO}_x$ ,  $\text{Eu}_2\text{TiO}_4$ , and  $\text{Eu}_3\text{Ti}_2\text{O}_7$  were produced<sup>2</sup> by heating proper proportions of  $\text{TiO}_2$ -,  $\text{Eu}_2\text{O}_3$ -, and Ti-metal powder at  $1400^\circ\text{C}$ . Phase identification was carried out by x-ray powder diffraction.<sup>2</sup> All absorbers contained 15–20  $\text{mg}/\text{cm}^2$  of material.

For the measurements at  $T \leq 4.2$  K, the absorbers were immersed in liquid helium. The pressure above the liquid-helium bath was controlled by a manostat capable of maintaining the bath temperature to better than 0.05 K. For  $T > 4.2$  K, the samples were heated above liquid-helium temperature by a temperature controller with a stability of about 0.1 K.

### IV. $\text{EuTiO}_x$

#### A. Mössbauer spectra of $\text{EuTiO}_x$ ( $2.68 \leq x \leq 3$ )

We have measured the Mössbauer spectra of  $\text{EuTiO}_x$  for  $x = 2.68, 2.70, 2.80, 2.85, 2.87, 2.91, 2.93, 2.97$ , and 3 at the temperatures of 300, 4.2,

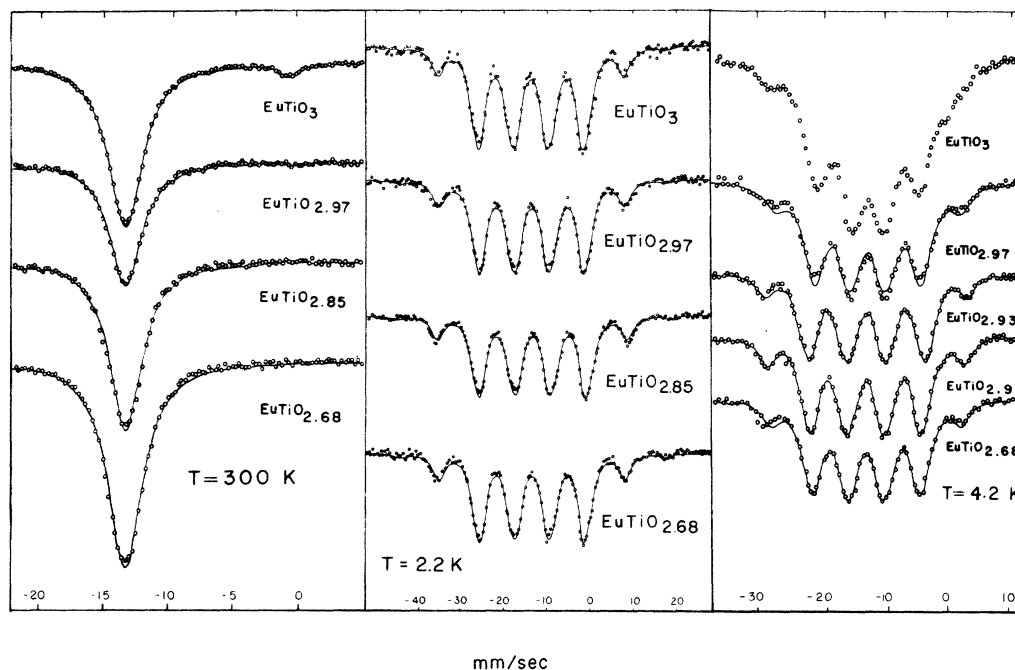


FIG. 3. Mössbauer spectra of  $\text{EuTiO}_x$  ( $2.68 \leq x \leq 3$ ) at 300, 2.2, and 4.2 K.

3.9, 3.7, 3.2, 2.6, and 2.2 K. Typical results are shown in Fig. 3.

The isomer shift was found to be  $-13.4 \pm 0.05$  mm/sec for all values of  $x$ , in agreement with Berkooz's result<sup>9</sup> of  $-13.5 \pm 0.1$  mm/sec for  $\text{EuTiO}_3$ .

At room temperature the spectra consists of a single line (paramagnetic state) which could be fitted with a Lorentzian with full width at half-maximum (FWHM) of about 3 mm/sec; no indication of quadrupole splitting was noted.

At 2.2 K all spectra show a magnetic structure (magnetically ordered state) which could be satisfactorily fitted with a single hyperfine field and a linewidth of about 2.8 mm/sec. The  $g$ -factor ratio of the two nuclear states was fixed to be 0.53.<sup>10</sup> The value of  $H_{\text{hf}}$  extrapolated to 0 K was  $325 \pm 7$  kOe for all values of  $x$ .

The magnetization curves for various values of  $x$  were slightly different, but no simple dependence on  $x$  was noted.<sup>11</sup> All samples ordered magnetically at the temperature of  $5.5 \pm 0.2$  K.

The spectra in the range  $2.68 \leq x < 2.97$  are quite similar for all temperatures and have the typical appearance of cubic  $\text{Eu}^{2+}$  spectra. No evidence of  $\text{Eu}^{3+}$  could be observed within this range.

For  $x = 2.97$  and  $x = 3$ , the spectra show evidence of  $\text{Eu}^{3+}$  impurity (about 1% for  $x = 2.97$  and 3% for  $x = 3$ ) which is revealed by the peak near zero velocity. For these same values of  $x$ , and for  $T \approx 4$  K, the appearance of the spectra is somewhat

atypical (with the four central peaks of different height).

It may be noticed that anomalous spectra only occur in samples with some  $\text{Eu}^{3+}$  impurity and at temperatures greater than 3.7 K. Groll<sup>12</sup> has observed a similar anomaly just below the critical temperature in  $\text{EuO}$  samples which contained observable amounts of  $\text{Eu}^{3+}$  impurity, and attributes the effect to critical superparamagnetism. Our effect, however, extends too far below the transition temperature to be explained by critical superparamagnetism. An alternative explanation could be that both  $\text{Eu}^{2+}$  and  $\text{Eu}^{3+}$  are present in the same crystalline phase as suggested by phase studies,<sup>3</sup> and that  $\text{Eu}^{3+}$  affects the local environment of  $\text{Eu}^{2+}$ , causing a spread in the values of  $H_{\text{hf}}$ .

#### B. Magnetic properties of $\text{EuTiO}_3$

Our determination of the magnetic transition temperature ( $T_N = 5.5 \pm 0.2$  K) can be considered to be in agreement with the magnetic measurement value of 5.3 K.<sup>2</sup> Susceptibility measurements showed that  $\text{EuTiO}_3$  is one of the few antiferromagnets with a positive Curie-Weiss constant of  $\Theta_C = 3.8$  K.<sup>2</sup> Neutron-diffraction results<sup>2</sup> at low temperature have shown that  $\text{EuTiO}_3$  has a type-G antiferromagnetic structure, i.e., the six nn's have opposite spins while the 12 nnn's have parallel spins. From these data, using the molecular-field theory, one can derive the nn and nnn exchange constants  $J_1$  and  $J_2$  from the equations:

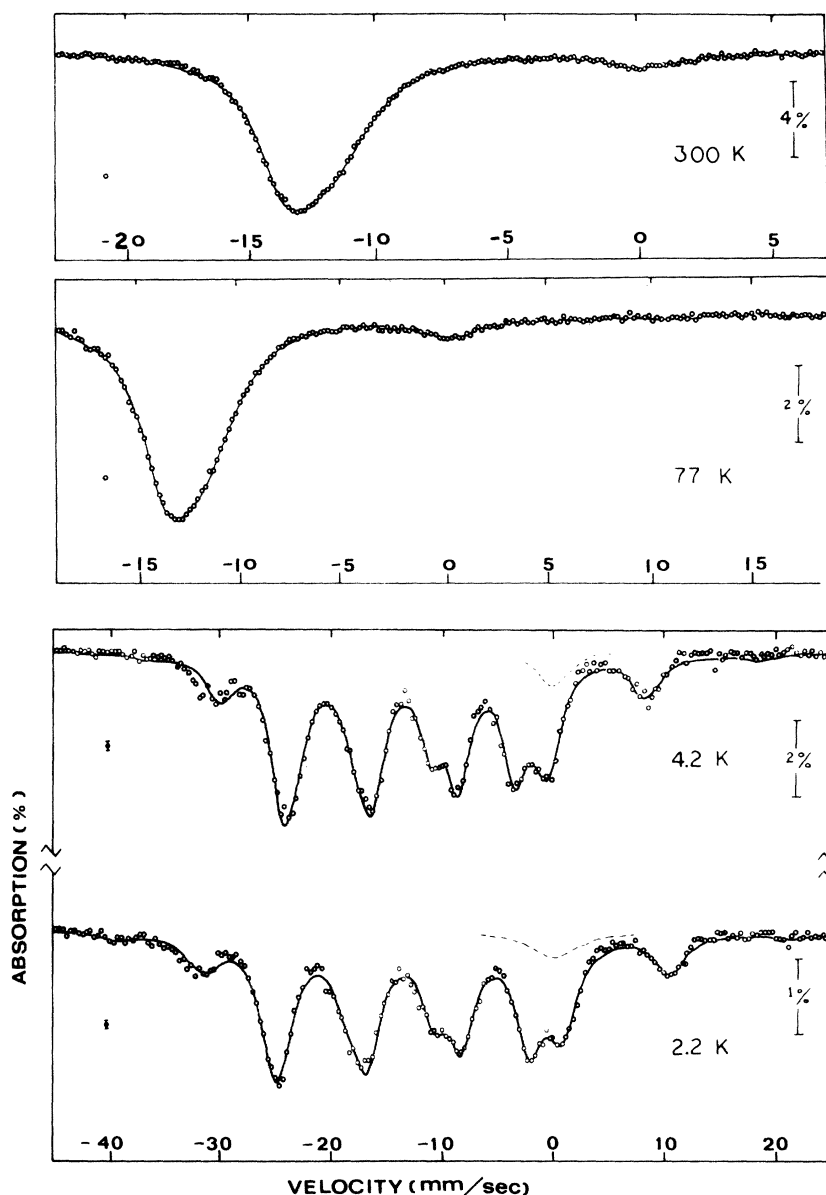


FIG. 4. Mössbauer spectra of  $\text{Eu}_2\text{TiO}_4$  at 300, 77, 4.2 and 2.2 K. The dotted curves indicate the  $\text{Eu}^{3+}$  peaks.

$$T_N = \frac{2S(S+1)}{3k}(-6J_1 + 12J_2) = 5.5 \text{ K}, \quad (6)$$

$$\Theta_C = \frac{2S(S+1)}{3k}(6J_1 + 12J_2) = 3.8 \text{ K},$$

where  $k$  is the Boltzmann constant and  $S = \frac{7}{2}$  for  $\text{Eu}^{2+}$ . One obtains<sup>13</sup>

$$J_1/k = -0.014 \text{ K}, \quad (7)$$

$$J_2/k = +0.037 \text{ K}.$$

The value of  $J_1/k$  is very much smaller than that of  $\text{EuO}$  ( $\sim 0.75 \text{ K}$ )<sup>5</sup> and  $\text{EuS}$  ( $\sim 0.2 \text{ K}$ )<sup>5</sup> despite the fact that the nn distance in  $\text{EuTiO}_3$  ( $3.9 \text{ \AA}$ ) is between that of  $\text{EuO}$  ( $3.63 \text{ \AA}$ ) and  $\text{EuS}$  ( $4.2 \text{ \AA}$ ). Furthermore, our recent studies have shown that  $\text{EuLiH}_3$

[which has the same perovskite structure and similar lattice constant ( $3.79 \text{ \AA}$ ) as that of  $\text{EuTiO}_3$  ( $3.90 \text{ \AA}$ )] is ferromagnetic with a high  $T_C = 37.6 \text{ K}$  with  $J_1/k \sim 0.8 \text{ K}$  and  $J_2/k \sim 0 \text{ K}$ .<sup>14</sup>

The difference between the values of  $J_1$  in these substances cannot depend on the difference of nn distances—which are practically the same in all cases—but can be attributed to variations in crystal-field splitting, according to Eqs. (1), (3), and (5) and to Fig. 2. In fact, if the  $10Dq$  of  $\text{EuTiO}_3$  were smaller than that of  $\text{EuO}$ ,  $\text{EuS}$ ,<sup>6</sup> and  $\text{EuLiH}_3$ ,<sup>15</sup> the value of  $U$  would be larger and that of  $J_1$  would be smaller, as observed.

Unfortunately, this explanation cannot be tested by direct comparison with experiment because the

$10Dq$  of  $\text{EuTiO}_3$  has not been measured. For a theoretical test, we have computed the  $10Dq$  of all the above substances, using an infinite lattice point-charge model (dipole terms do not contribute because of inversion symmetry). The results<sup>16</sup> obtained with this model support this suggestion, since the calculated  $|10Dq|$  for  $\text{EuTiO}_3$  is indeed an order of magnitude smaller than the  $|10Dq|$  of the other compounds.

#### V. $\text{Eu}_2\text{TiO}_4$

##### A. Quadrupole splitting in $\text{Eu}_2\text{TiO}_4$

Mössbauer spectra of  $\text{Eu}_2\text{TiO}_4$  were measured at 300, 77, 8.1, 7.5, 5.7, 4.2, 3.6, 3.2, 2.5, and 2.2 K. Typical results are shown in Fig. 4. The weak peak near zero velocity shows the presence of about 4%  $\text{Eu}^{3+}$  impurity in our sample.

At 300 and 77 K, the spectra can be interpreted in terms of pure quadrupole effects. Since the  $\text{Eu}^{2+}$  site has fourfold symmetry, the EFG asymmetry parameter  $\eta$  is zero, and the  $z$  axis of the EFG is in the direction of the crystal  $c$  axis. We can thus use the Hamiltonian

$$\frac{e^2qQ}{4I(2I-1)} [3I_z^2 - I(I+1)], \quad (8)$$

where  $eq = V_{zz}$  is the EFG component along the fourfold  $c$  axis,  $eQ$  is the nuclear quadrupole moment, and  $I$  the nuclear spin.

At low temperatures, one observes the effect of a hyperfine magnetic field,  $H_{\text{hf}}$ , which in general has a different direction from the  $c$  axis. Then the Hamiltonian can be approximately written as<sup>17</sup>

$$\frac{e^2q_{\text{eff}}Q}{4I(2I-1)} [3I_z^2 - I(I+1)] - g\mu_N H_{\text{hf}} I_z, \quad (9)$$

where  $q_{\text{eff}} = q(3\cos^2\theta - 1)/2$  and  $\theta$  is the angle between  $H_{\text{hf}}$  and  $c$  axis.  $q_{\text{eff}}$  is equal to  $q$  when  $\theta$  is equal to zero and smaller otherwise.

The data for  $T \leq 4.2$  K were fitted using Eq. (9) in terms of the parameters  $H_{\text{hf}}$ ,  $e^2q_{\text{eff}}Q_0$ ,  $R = Q_1/Q_0$ , and amplitude, FWHM, and isomer shift for  $\text{Eu}^{2+}$  and  $\text{Eu}^{3+}$ . We obtained in this manner

$$\begin{aligned} e^2q_{\text{eff}}Q_0 &= -190 \pm 5 \text{ MHz}, \\ R = Q_1/Q_0 &= 1.34 \pm 0.03. \end{aligned} \quad (10)$$

Our value of  $R$  is slightly larger than those reported by Stachel *et al.*<sup>18</sup> ( $1.28 \pm 0.05$ ) and Kalvius *et al.*<sup>19</sup> ( $1.30 \pm 0.05$ ). However, our result should be more reliable since these authors used compounds with low symmetry at the Eu site (thus  $\eta \neq 0$ ), but assumed  $\eta = 0$  in their analysis.

The spectra at 300 and 77 K were fitted by Eq. (8) with the parameter  $R$  fixed at the value 1.34, found from the low-temperature results. We obtained in this manner  $e^2qQ_0 = -189 \pm 2$  MHz. Thus,

within the experimental errors, we can say that  $q = q_{\text{eff}}$ , independent of temperature, as expected for a pure lattice contribution. Using the value  $Q_0 = (1.14 \pm 0.05) \times 10^{-24} \text{ cm}^2$ ,<sup>20</sup> we obtain  $q = q_{\text{eff}} = (-4.75 \pm 0.2) \times 10^{24} \text{ cm}^{-3}$ .

The isomer shift relative to  $\text{Eu}_2\text{O}_3$  at room temperature is  $-12.8 \pm 0.1 \text{ mm/sec}$ <sup>21</sup> for  $\text{Eu}^{2+}$  and remains constant, within the experimental error throughout the temperature range in this work. The extrapolated zero-degree hyperfine field is  $305 \pm 3 \text{ kOe}$ .<sup>21</sup>

Since the  $\text{Eu}^{2+}$  ion, neglecting  $d$  admixture, is spherically symmetrical, the lattice contribution to the EFG at the nucleus should be predominant. Thus, we have attempted to compute the lattice contribution to the parameter  $q$  by performing a lattice sum. The contribution from  $5d$  admixture can be estimated to be small,<sup>11</sup> and covalency effects, which are difficult to evaluate have been entirely neglected. The basic formula is simply

$$q_{\text{calc}} = (1 - \gamma_\infty)q_{\text{lat}} = (1 - \gamma_\infty) \sum_i e_i (3z_i^2 - r_i^2/r_i^5), \quad (11)$$

where  $\gamma_\infty \approx -80$  is the antishielding factor,<sup>22</sup> and  $(x_i, y_i, z_i)$  are the coordinates of the charge  $e_i$  with respect to the position where EFG is being calculated. The summation should include all ions in a macroscopic crystal, but one hopes that, in practice, it will converge rapidly to the infinite lattice value when a fairly large number of ions are included. Using the conventional method of calculating contributions from ions inside larger and larger spheres, we found no rapid convergence; however, rapid convergence was obtained with the method of chargeless clusters<sup>23-25</sup> which employs clusters of neutral unit cells with centers within the sphere. The calculated value was  $q_{\text{calc}} = -3.3 \times 10^{24} \text{ cm}^{-3}$ , comparable to the measured value of  $q = -4.75 \times 10^{24} \text{ cm}^{-3}$ . The agreement also confirms that the small  $5d$  admixture and covalency are probably not of major importance.

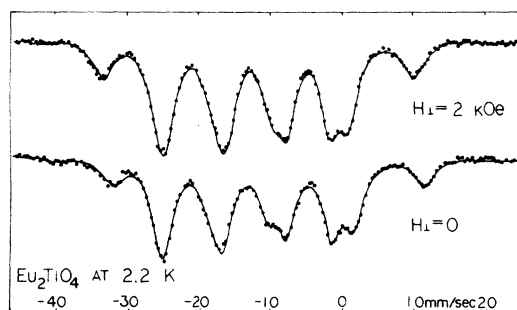


FIG. 5. Mössbauer spectra of  $\text{Eu}_2\text{TiO}_4$  at 2.2 K with and without a 2-kOe external magnetic field applied perpendicular to the  $\gamma$ -rays direction.

B. Magnetic properties of  $\text{Eu}_2\text{TiO}_4$ 

Since all the spectra of  $\text{Eu}_2\text{TiO}_4$  could be satisfactorily fitted with lines of narrow width of about 2.6 mm/sec, we can assume that the measured hyperfine fields are proportional to the magnetization. The ordering temperature of  $\text{Eu}_2\text{TiO}_4$  was found to be  $7.8 \pm 0.2$  K.

From the expected temperature independence of the EFG, and the experimental results  $q = q_{\text{eff}}$ , we conclude that the magnetic ordering of  $\text{Eu}_2\text{TiO}_4$  is collinear, with the magnetization along the  $c$  axis.

It was also found that an external applied magnetic field of 2 kOe reduces the  $e^2q_{\text{eff}}Q_0$  value at low temperatures from  $-190$  to  $-80$  MHz (Fig. 5). Since this weak applied field was sufficient to change the direction of magnetization away from the randomly oriented  $c$  axes of our powder sample,  $\text{Eu}_2\text{TiO}_4$  is likely to be ferromagnetic. Bulk magnetic measurements performed on the same sample used in the Mössbauer studies have in fact confirmed that  $\text{Eu}_2\text{TiO}_4$  is ferromagnetic with  $T_C = 9 \pm 2$  K and  $\Theta_C = 10 \pm 2$  K.<sup>26</sup>

From Table I, using molecular-field theory, one has

$$T_C = \Theta_C = \frac{2S(S+1)}{3k} (4J_{11} + 4J_{12} + J_{13} + 4J_{21} + 4J_{22}) . \quad (12)$$

We shall assume that the nnn interactions are the same as for  $\text{EuTiO}_3$ . Thus

$$J_{21}/k \approx J_{22}/k \approx J_2/k = 0.037 \text{ K} . \quad (13)$$

We have tried to estimate the relative importance of the nn exchange interaction assuming that they are caused by  $5d$  admixture. For this we have computed the  $5d$  crystal-field splittings under tetragonal symmetry using the infinite lattice point-charge model, with the results shown in Fig. 2.

Notice that the over-all splitting in  $\text{Eu}_2\text{TiO}_4$  is much larger than that of  $\text{EuTiO}_3$ . Since the  $|3z^2 - r^2\rangle$  state is high, one expects that

$$J_{13}/k \approx 0 . \quad (14)$$

Then from Eq. (12) we obtain

$$(J_{11} + J_{12})/k = 0.11 \text{ K} . \quad (15)$$

Furthermore, it is likely that  $J_{12} > J_{11}$ , since the connecting  $5d$  state is lower in energy and the nn separation is shorter for  $J_{12}$ . It is interesting to note that  $J_{12}$  of  $\text{Eu}_2\text{TiO}_4$  is much larger than  $J_1$  of  $\text{EuTiO}_3$ , consistent with the difference in the  $5d$  crystal splitting (Fig. 2).

VI.  $\text{Eu}_3\text{Ti}_2\text{O}_7$ A. Mössbauer spectra of  $\text{Eu}_3\text{Ti}_2\text{O}_7$ 

The Mössbauer spectrum of  $\text{Eu}_3\text{Ti}_2\text{O}_7$  at 2.3 K is shown in Fig. 6. The spectrum was fitted considering that there are two inequivalent sites of  $\text{Eu}^{2+}$  and some  $\text{Eu}^{3+}$  impurity. The  $\text{Eu}_2\text{TiO}_4$  site of tetragonal symmetry ( $\eta = 0$ ) has evident quadrupole interaction and the  $\text{EuTiO}_3$  site has negligible quadrupole splitting; the  $\text{Eu}^{3+}$  impurity contributes a single Lorentzian peak. The best fit was obtained for a ratio of about 2/1 of  $\text{Eu}_2\text{TiO}_4$  sites to  $\text{EuTiO}_3$  sites, consistent with the crystal structure, assuming both sites have the same Debye temperature.

The isomer shifts (i. s.) of the two sites have very different values as can be seen in Fig. 6. The i. s. values at 2.3 K are  $-12.6 \pm 0.2$  mm/sec ( $\text{Eu}_2\text{TiO}_4$  site) and ( $\text{EuTiO}_3$  site)  $-13.8 \pm 0.2$  mm/sec,<sup>27</sup> which are similar to the values for  $\text{Eu}_2\text{TiO}_4$  and  $\text{EuTiO}_3$ , respectively.

The measured  $e^2q_{\text{eff}}Q_0 = -150 \pm 10$  MHz for the  $\text{Eu}_2\text{TiO}_4$  sites at low temperatures is close to the

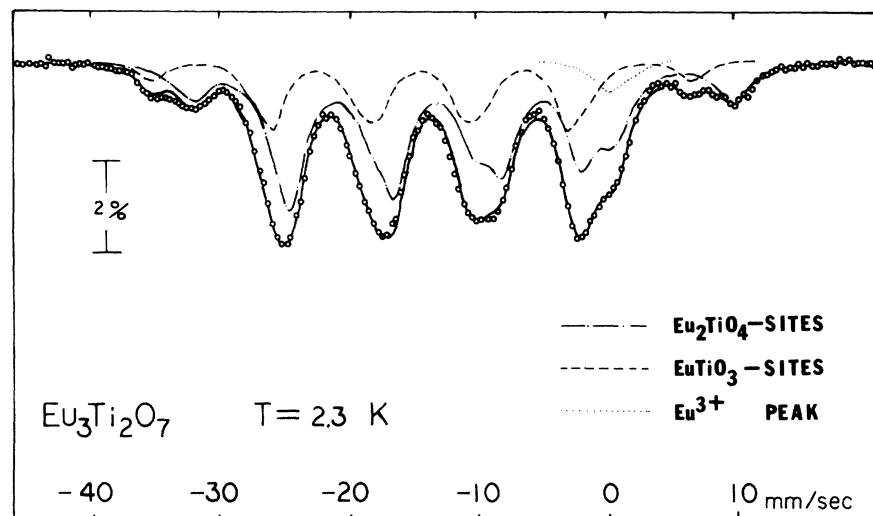


FIG. 6. Mössbauer spectrum of  $\text{Eu}_3\text{Ti}_2\text{O}_7$  at 2.3 K.

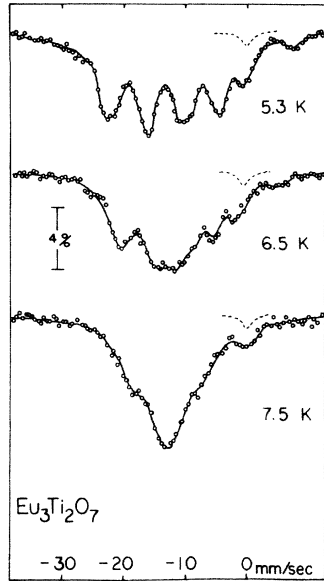


FIG. 7. Mössbauer spectra of  $\text{Eu}_3\text{Ti}_2\text{O}_7$  at 5.3, 6.5, and 7.5 K. The dotted curves indicate the  $\text{Eu}^{3+}$  peaks.

value  $e^2qQ_0 = -160 \pm 3$  MHz at room temperature. Therefore  $\text{Eu}_3\text{Ti}_2\text{O}_7$  is also likely to have collinear spin structure along the  $c$  axis. Using the charge-less cluster method described in Sec. V A, we obtained the calculated values of  $e^2qQ_0$  ( $\text{Eu}_2\text{TiO}_4$  site)  $= -115$  MHz and  $e^2qQ_0$  ( $\text{EuTiO}_3$  site)  $= -5$  MHz. The former agrees with the measured value in magnitude and sign. The latter shows that the quadrupole interaction at the  $\text{EuTiO}_3$  site should be unmeasurably small, in agreement with the good fit obtained by using a pure magnetic Hamiltonian for the site.

The extrapolated zero-degree hyperfine fields for the two sites are similar to those of  $\text{EuTiO}_4$  and  $\text{EuTiO}_3$ , respectively.<sup>27</sup> As the temperature is raised,  $H_{\text{hf}}$  ( $\text{EuTiO}_3$  site) decreases more rapidly than  $H_{\text{hf}}$  ( $\text{Eu}_2\text{TiO}_4$  site) as shown in Fig. 7. The reduced hyperfine fields of the two sites versus  $T$  are shown in Fig. 8. As we have assumed the proportionality between the hyperfine field and the sublattice magnetization, the ordering temperature was found to be  $8 \pm 0.3$  K.

#### B. Magnetic properties of $\text{Eu}_3\text{Ti}_2\text{O}_7$

Since only two hyperfine fields can be observed in the spectra of  $\text{Eu}_3\text{Ti}_2\text{O}_7$  at low temperatures, one concludes that there are only two magnetically inequivalent sites in the magnetically ordered state. The measured EFG indicates that the spin structure is most likely collinear along the  $c$  axis. The magnetization of the  $\text{Eu}_2\text{TiO}_4$  sites has a normal temperature dependence whereas that of  $\text{EuTiO}_3$  sites is unusual (Fig. 8).

The information about the nn's and the nnn's is shown in Fig. 1 and in Table I. It should be emphasized that the geometrical arrangement of the nn's and nnn's is the same as for  $\text{Eu}_2\text{TiO}_4$  and  $\text{EuTiO}_3$ . The calculated  $5d$  splittings are also similar to those of  $\text{Eu}_2\text{TiO}_4$  and  $\text{EuTiO}_3$  (Fig. 2). Therefore, the exchange interactions can be expected to have nearly the same values as the corresponding ones in  $\text{Eu}_2\text{TiO}_4$  and  $\text{EuTiO}_3$  [Eqs. (7) and (13)–(15)].

With these values, a calculation of the free energy of  $\text{Eu}_3\text{Ti}_2\text{O}_7$  at  $T=0$  using Heisenberg model and assuming a collinear spin structure shows that ferromagnetic ordering has the lowest energy.<sup>11</sup> This can be understood considering that the  $\text{Eu}_2\text{TiO}_4$  layer orders ferromagnetically because of the large positive values of  $J_{11} + J_{12}$ , and that the antiferromagnetic tendency of  $\text{EuTiO}_3$  is overcome by the large effective field produced by the  $\text{Eu}_2\text{TiO}_4$  sites at the  $\text{EuTiO}_3$  site.

Using the molecular-field theory,<sup>28</sup> the effective fields at the  $\text{EuTiO}_3$  sites ( $a$  sites) and  $\text{Eu}_2\text{TiO}_4$  sites ( $b$  sites) can be written as<sup>28</sup>

$$\vec{H}_a = \frac{2S}{g\mu_B} (\gamma_{aa}\vec{\sigma}_a + \gamma_{ab}\vec{\sigma}_b) + \vec{H}_0, \quad (16)$$

$$\vec{H}_b = \frac{2S}{g\mu_B} (\gamma_{ba}\vec{\sigma}_a + \gamma_{bb}\vec{\sigma}_b) + \vec{H}_0,$$

where  $H_0$  is the external magnetic field,  $g\mu_B S\sigma_a$  and  $g\mu_B S\sigma_b$  are the average magnetic moment of the two  $\text{Eu}^{2+}$  sites,  $S = \frac{7}{2}$ ,  $0 \leq \sigma_a, \sigma_b \leq 1$  are the reduced magnetizations,  $\gamma_{aa}$  is the sum of interactions at the  $a$  site due to  $a$  sites,  $\gamma_{ab}$  is the sum of interactions at the  $a$  site due to  $b$  sites, etc. Referring to Fig. 1 and Table I, one has<sup>28</sup>

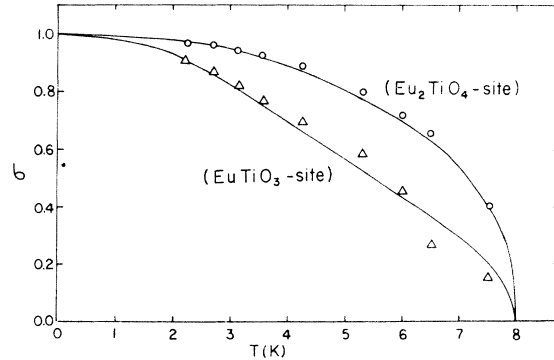


FIG. 8. Temperature dependences of the reduced magnetizations of the two inequivalent sites of  $\text{Eu}_3\text{Ti}_2\text{O}_7$ . The error in  $\sigma$  is about 2% at low temperature and 5% at high temperature. The solid curves are the molecular-field theory results.



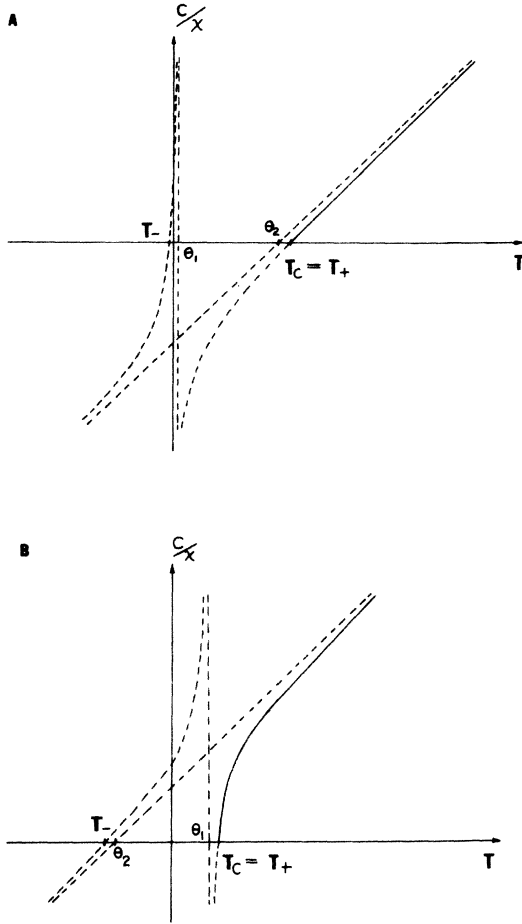


FIG. 9. Inverse susceptibility of (a)  $\text{Eu}_3\text{Ti}_2\text{O}_7$  and (b) typical case. The solid curves are the measurable part.

$$\begin{aligned}\gamma_{aa} &= 4J_1 + 4J_2, \\ \gamma_{ab} &= 2\gamma_{ba} = 2(J_{13} + 4J_{22}), \\ \gamma_{bb} &= 4J_{11} + 4J_{12} + 4J_{21},\end{aligned}\quad (17)$$

and  $\sigma_a$ ,  $\sigma_b$  can be obtained by solving the coupled equations:

$$\begin{aligned}\sigma_a &= B_S(g\mu_B SH_a/kT), \\ \sigma_b &= B_S(g\mu_B SH_b/kT).\end{aligned}\quad (18)$$

Letting  $H_0 = 0$ , the expression for the ordering temperature  $T_C$  can be obtained as

$$T_C = T_+ = \frac{2S(S+1)}{3k} \{ \gamma_{aa} + \gamma_{bb} + [(\gamma_{aa} - \gamma_{bb})^2 + 2\gamma_{ab}^2]^{1/2} \}.\quad (19)$$

Using the values for  $\text{EuTiO}_3$  and  $\text{Eu}_2\text{TiO}_4$ , from

Eqs. (7), (13), and (15), one obtains

$$\gamma_{aa}/k = 0.1 \text{ K}, \quad \gamma_{ab}/k = 0.3 \text{ K}, \quad \gamma_{bb}/k = 0.59 \text{ K}, \quad (20)$$

and  $T_C = 7 \text{ K}$ . This value is only slightly smaller than the measured value of about 8 K. In order to have better agreement with the experimental results, we adjust slightly to

$$\gamma_{aa}/k = 0.1 \text{ K}, \quad \gamma_{ab}/k = 0.4 \text{ K}, \quad \gamma_{bb}/k = 0.64 \text{ K}, \quad (21)$$

and  $T_C = 8 \text{ K}$  is obtained. The reduced sublattice magnetization curves, calculated numerically for the adjusted values of Eq. (21) are shown in Fig. 8 together with the experimental results. The agreement is satisfactory.

From Eq. (18) the inverse magnetic susceptibility can be calculated as

$$c/\chi = T - \Theta_2 - \frac{(T_+ - \Theta_1)(T_+ - \Theta_2)}{T - \Theta_1}, \quad (22)$$

where

$$T_+ = T_C,$$

$$T_- = \frac{2S(S+1)}{3k} \frac{1}{2} \{ \gamma_{aa} + \gamma_{bb} - [(\gamma_{aa} - \gamma_{bb})^2 + 2\gamma_{ab}^2]^{1/2} \},$$

$$\Theta_1 = \frac{2S(S+1)}{3k} \frac{1}{3} [2\gamma_{aa} + \gamma_{bb} - 2\gamma_{ab}],$$

$$\Theta_2 = \frac{2S(S+1)}{3k} \frac{1}{3} [\gamma_{aa} + 2\gamma_{bb} + 2\gamma_{ab}].$$

The  $1/\chi$  vs  $T$  relation for  $\text{Eu}_3\text{Ti}_2\text{O}_7$ , given by Eq. (22) with the numerical values of  $T_+$  and  $\Theta_{1,2}$  determined from Eq. (21), is plotted in Fig. 9(a). From this figure we see that the ordering temperature  $T_C$  is very near  $\Theta_2$ , a situation which is uncommon for typical ferrimagnet [Fig. 9(b)], but is in agreement with the result of bulk magnetic measurements which showed  $T_C = 8.5 \pm 2 \text{ K}$  and  $\Theta_2 = 9 \pm 2 \text{ K}$ .<sup>26</sup>

Ferrimagnets with positive exchange interaction between inequivalent sites are uncommon.<sup>28</sup> All the indications we have show that  $\text{Eu}_3\text{Ti}_2\text{O}_7$  is a ferrimagnet with ferromagnetic ordering due to  $\gamma_{ab} > 0$ .

#### ACKNOWLEDGMENTS

We thank Dr. G. J. McCarthy of Penn State University, Material Research Laboratory for kindly providing us with the samples used in this investigation. We are also grateful to helpful discussions with Dr. W. T. Oosterhuis, Dr. J. O. Artman, and Dr. B. Window.

<sup>†</sup>Work supported in part by the National Science Foundation and the Office of Naval Research.

\*Present address: Department of Physics, The Johns Hopkins University, Baltimore, Md.

<sup>1</sup>B. T. Matthias, R. M. Bozorth, and J. H. Van Vleck, Phys. Rev. Lett. **7**, 160 (1961).

<sup>2</sup>T. R. McGuire, M. W. Shafer, R. J. Joenk, H. A. Alperin, and S. J. Pickart, J. Appl. Phys. **31**, 981 (1966).

- <sup>3</sup>G. J. McCarthy, W. B. White, and R. Roy, *Inorg. Nucl. Chem.* **31**, 329 (1969).
- <sup>4</sup>J. B. Goodenough, *Magnetism and the Chemical Bond* (Interscience, New York, 1963).
- <sup>5</sup>S. Methfessel and D. C. Mattis, in *Handbuch der Physik*, edited by S. Flugge (Springer-Verlag, Berlin, 1968), Vol. 18, No. 1, p. 389.
- <sup>6</sup>J. O. Dimmock, *IBM J. Res. Dev.* **14**, 301 (1970).
- <sup>7</sup>T. Kasuya, *IBM J. Res. Dev.* **14**, 214 (1970).
- <sup>8</sup>T. Kasuya and A. Yanase, *Rev. Mod. Phys.* **40**, 684 (1964).
- <sup>9</sup>O. Berkooz, *J. Phys. Chem. Solids* **30**, 1763 (1969).
- <sup>10</sup>V. S. Shirley, in *Hyperfine Structure and Nuclear Radiations*, edited by E. Matthias and D. A. Shirley (North-Holland, Amsterdam, 1968), p. 1014.
- <sup>11</sup>C. L. Chien, thesis (Carnegie-Mellon University, 1973) (unpublished).
- <sup>12</sup>G. Groll, *Z. Phys.* **243**, 60 (1970).
- <sup>13</sup>Reference 2 obtained  $J_1/k = -0.02$  K and  $J_2/k = 0.04$  K by using a slightly different expression for  $T_N$ , and  $T_N = 5.3$  K was used.
- <sup>14</sup>C. L. Chien and J. E. Greedan, *Phys. Lett. A* **36**, 197 (1971).
- <sup>15</sup>J. E. Greedan, *J. Phys. Chem. Solids* **32**, 1039 (1971).
- <sup>16</sup>C. L. Chien, S. DeBenedetti, and F. de S. Barros, *Int. J. Magn.* (to be published).
- <sup>17</sup>E. Matthias, W. Schneider, and R. M. Steffan, *Phys. Rev.* **125**, 261 (1962).
- <sup>18</sup>M. Stachel, S. Hufner, G. Crecelius, and D. Quitmann, *Phys. Rev.* **186**, 355 (1969).
- <sup>19</sup>G. M. Kalvius, G. K. Shenoy, G. J. Ehnholm, T. E. Katile, O. V. Lounasmaa, and P. Reiveri, *Phys. Rev.* **187**, 1503 (1969).
- <sup>20</sup>G. Guthohrlein, *Z. Phys.* **214**, 332 (1968).
- <sup>21</sup>C. L. Chien and F. de S. Barros, *Phys. Lett. A* **38**, 427 (1972).
- <sup>22</sup>R. E. Watson and A. J. Freeman, *Phys. Rev.* **135**, A1209 (1964).
- <sup>23</sup>R. H. Wood, *J. Chem. Phys.* **32**, 1690 (1960).
- <sup>24</sup>J. O. Artman and J. C. Murphy, *Phys. Rev.* **135**, A1622 (1964).
- <sup>25</sup>J. O. Artman, *Mössbauer Effect Methodology*, edited by I. J. Gruverman (Plenum, New York, 1972), Vol. 7.
- <sup>26</sup>J. E. Greedan and G. J. McCarthy, *Mat. Res. Bull.* **7**, 531 (1970).
- <sup>27</sup>C. L. Chien, S. DeBenedetti and F. de S. Barros, *Phys. Lett. A* **44**, 178 (1973).
- <sup>28</sup>J. S. Smart, *Effective Field Theories of Magnetism* (Saunders, Philadelphia, 1966).